Maintaining the closed magnetic-field-line topology of a field-reversed configuration (FRC) with the addition of static transverse magnetic fields

S.A. Cohen, Princeton University, Plasma Physics Laboratory, Princeton, NJ 08543 and
R. D. Milroy, University of Washington, Redmond Plasma Physics Laboratory, Redmond, WA 98052

Abstract

The effects on magnetic-field-line structure of adding various static transverse magnetic fields to a Solov'ev-equilibrium field-reversed configuration is examined. It is shown that adding fields that are anti-symmetric about the axial mid-plane maintains the closed field-line structure, while adding fields with planar or helical symmetry opens the field structure. Anti-symmetric modes also introduce pronounced shear.

I. Introduction

Magnetic field lines are closed. Where closure occurs is of importance to many physical phenomena in solar, planetary, and fusion plasma physics. It is well known that a magnetic-field geometry may be markedly changed by the application of small additional magnetic fields. In this article we concentrate on the effects of small, primarily transverse magnetic fields added to a particular magnetic-field geometry, the field-reversed configuration (FRC).[1] Our interest in this device is based on its relevance to fusion research. The goal is to find generic properties of transverse fields that do not significantly change the FRC's closed field structure.

The FRC is an example of a self-organized plasma wherein a strong internal toroidal current, in combination with the axial magnetic field from a linear solenoidal coil, generates a closed poloidal magnetic-field structure inside the solenoid, see Figure 1. We ask whether the FRC's magnetic-field-line structure must open when a transverse magnetic field is added. (Transverse means perpendicular to the FRC's major axis. In the jargon of magnetic-fusion research, an *open* field line intersects the external solenoidal coil or a material structure, such as the vacuum-vessel wall, of the FRC device, or extends outside the solenoidal coil; a *closed* field line does not.)

Added transverse fields may be constant or time varying. Time-varying fields are particularly important for the rotating magnetic field (RMF) current-generation method[2] developed in rotamak devices.[3] However, the purely geometrical analysis presented here, the essential first step in examining field closedness, is restricted to temporally constant magnetic fields. Time variation of the transverse field is only explicitly included when ascribing field-line identity. Particle and energy confinement, clearly connected to field-line closedness, cannot be properly addressed by this analysis. They require a self-consistent many-particle treatment, not a purely geometrical one.

In small experiments (such as Ref. 2), the RMF method has been successful in generating and sustaining plasmas, as well as driving currents and reversing the axial field. Larger experiments,[4] at higher power, are in progress. These may produce higher temperature plasmas, far more susceptible to particle and energy losses on open field lines. This possibility strongly motivates the present field-line closure analysis.

The study of field-line closure for FRC-like plasmas with transverse applied fields has a long history. First in planetary sciences[5] and then in fusion research,[6,7] it was appreciated that opening of some field lines resulted from the addition of a uniform

transverse field to FRC-like configurations. A later paper[8] on the rotamak showed that the standard RMF mode caused a shift and tilt of the flux surfaces. Subsequent rigorous analyses[9,10] showed that all field lines actually opened. Even when a very small uniform transverse field was added, initially closed field lines unwound in spirals, eventually intersecting the device's boundaries.

In this paper we show that a particular small-amplitude transverse-field shape globally preserves the closedness of the field lines. By "*globally preserves"* we mean that a well-defined separatrix is maintained and that all field lines interior to the separatrix, save that through the X points, are closed inside the separatrix. These closedness-preserving (CP) transverse-field modes appear to be suitable for current drive and for more speculative applications, such as ion heating[11] and FRC stabilization.[12] Analyses of these are in progress.

In Section II we present a rigorous graphical proof showing CP for a particular anti-symmetric transverse mode (labeled the $\ell_- = 1$ for reasons that will become clear). The results are then generalized to other transverse modes including the closure-destroying standard RMF mode, the $\ell_+ = 0$. Field-line graphs, created by numerical integration with a predictor-corrector code, illustrate these analyses in Section III. Select results of Ref. 9 and 10 are duplicated for a Solov'ev equilibrium,[13] confirming that field line opening is the result of the $\ell_+ = 0$ commonly used in rotamak experiments. The numerical code is then used to corroborate the graphical proof for CP of the $\ell_- = 1$ mode. Novel shapes of the net field are seen which may be important to stability.

II. Examination of field-line closure by a graphical technique

For the graphical proof, we analyze the addition of a particular static, anti-symmetric, (predominantly) transverse magnetic field, $\mathbf{B}_{T-}$, to a Solov'ev-equilibrium FRC whose major axis is along the *z*-axis. The selected magnetic field, shown in Figure 2, could be created by currents in 5 pairs of parallel wires, oriented perpendicular to the *z* and *y* axes of the FRC, see Figure 3. Being a vacuum field, $\nabla \times \mathbf{B} = 0$. This field is described by the equation,

$$\mathbf{B}_{T-} = \mathbf{e}_y B_\tau f_-(z-z_0) + \mathbf{e}_z B_\pi g_-(z-z_0), \qquad (1)$$

where $\mathbf{e}_y$ and $\mathbf{e}_z$ are unit vectors in the *y* and *z* directions respectively, B_τ and B_π are (respectively) the amplitudes of the transverse and parallel components of the added

field, and f_- has odd parity about the z_0 plane. (r_0, z_0) is the location of the FRC's minor magnetic axis. In the absence of internal currents, once $B_\tau\, f_-(z\text{-}z_0)$ is specified, $B_\pi g_-(z\text{-}z_0)$ is uniquely determined by the conditions $\nabla\mathbf{x}\mathbf{B} = 0$ and $\nabla\cdot\mathbf{B} = 0$. Note that for anti-symmetric $f_-(z\text{-}z_0)$, the vector field, $\mathbf{e}_z\, B_\pi\, g_-(z\text{-}z_0)$ is also anti-symmetric, that is, it has odd parity in the sense that $\mathbf{B}_\pi$ points towards the $z = z_0$ plane on one side of that plane and away from it on the other.

To define the mode number ℓ, observe, from Figure 2b), that f_- is approximately described by Sin $k(z\text{-}z_0)$ in the region $-2 < z < 2$, where $k = 2\pi\ell/L$, L is the FRC's characteristic length, 2ℓ is the number of nodes within L, and we have set $z_0 = 0$. (In counting nodes, one lying on the boundary, the separatrix, has a value of 1/2.) The "–" subscript signifies anti-symmetry (odd parity) about the plane $z = z_0$; a "+" subscript would mean symmetric (even parity) about the $z = z_0$ plane.

For the following analysis we call the mode number $\ell_- = 1$, even though the nodes of f_- fall on the *z extrema* of the closed field lines being considered, not on the separatrix. (Perhaps more precisely, the mode should be called $\ell_- \approx 1$.) The numerical calculations described in Section III were done with the B field shown in Figure 2, not the Sin approximation.

Our goal is to show that the $\ell_- = 1$ mode preserves closedness. A sufficient condition to be CP will be noted later. This argument will show why the standard rotamak, with a symmetric [$f_+ = \text{Cos } k(z\text{-}z_0)$] spatially constant ($\ell_+ = 0$) or nearly constant ($0 < \ell_+ < 1$) transverse field is non-CP.

A. Graphing procedure: Anti-symmetric mode

Consider a closed flux surface (a field line, B_s) of a Solov'ev FRC. One of extent L in the *z* direction, centered at (r_0, z_0), and lying in the positive *y*-*z* plane is shown as the solid curve in Figure 4a). The main axial magnetic field, B_z, is in the +*z* direction. Note that $y = y_0 \neq r_0$ at $z\text{-}z_0 = \pm L/2$. Because the FRC is a toroid, the field line is not symmetric about the line $y = y_0$, while it is symmetric about the line $z = z_0$. By graphing this field line from point *a*, going 90° in a clockwise (CW) direction around the point (y_0, z_0), one arrives at point *b*. (Graphing means following a field line.)

Consider the addition (to the Solov'ev field, $\mathbf{B}_s$) of the small magnetic field described exactly in Figure 2, with approximate transverse amplitude shown in Fig 4b) and having half nodes at *a* and *a'*. The new graph, see dashed line in Figure 4a), shows that the net field line shifts in the *y* direction, away from the z-axis. [The field line moves further away from the *z* axis because B_τ adds to the FRC's transverse field, see figure 4c).] The field line consequently reaches point *c*, which lies above point *b*. The effect of the small parallel component of the added field, B_π, Figure 4c), is explicitly included in the graphing procedure. Now repeat the field-line-following procedure from point *a'*, but in a counterclockwise (CCW) direction around the point (y_0, z_0). Graphing *against* a vector field is performed by reversing the directions of all components of the FRC's Solov'ev field and of the added field, see Figures d) and e). The symmetry of the FRC's field and the anti-symmetry of the added field, makes this field-line-following procedure also arrive at *c*, where it connects with the first segment. [This is readily seen from the mirror symmetry of Figures 4c) and e).] The same graphing procedure, performed for the lower part of this flux surface, moves CCW from point *a* towards point *b'* and arrives at *c';* graphing from *a'*, proceeding CW, also arrives at *c'*. Thus, this flux surface remains closed, but grows in enclosed area.

Flux surfaces of shorter or longer length (compared to L) also remain closed, but their end points (*a* and *a'*) shift parallel to the *z*-axis. Further discussion on the related issue of field-line identity is deferred to later in this paper.

The mirror-image closed flux surface in the lower part of the *y*-*z* plane, Figure 4f), similarly remains closed with the addition of $\mathbf{B}_{T-}$, but its enclosed area shrinks because the added transverse field is anti-parallel to the FRC's field component in the *y* direction. Numerical integration will show more complex behavior near the O point than the simple shrinkage in area noted here.

For the $\ell = 1$ mode, a similar proof can be constructed for flux surfaces lying in the *x*-*z* plane, perpendicular to $\mathbf{B}_{T-}$. The anti-symmetric transverse field first lifts the field line out of its original plane and then, after crossing $z = z_0$, returns it to the original plane. To first order, the result is a tilt of the flux surface out of the original plane, see Figure 5a). By anti-symmetry, the flux surface remains closed. Figures 5b), 5c), and 5d) show the components of the FRC field, $\mathbf{B}_s$, and the added field at two points, *e* and *e'*, as well as the mirror-reflected components at *e'* for mapping in the CW direction. Numerical integration will show that the change in flux surface shape is more than a simple tilt: the

nested, tilted, flux-surface structure develops curvature and shear, which may be important to stability.

To assess the effect of adding an anti-symmetric field to FRC flux surfaces lying in neither the *x-z* nor the *y-z* planes, decompose the anti-symmetric $\mathbf{B}_{T-}$ field into components parallel and perpendicular to the plane of the flux surface. Next, sequentially perform the field-line-following procedure, first for the parallel components, then for the perpendicular ones. During these two steps, closure of the net field is maintained because the components are also anti-symmetric. This completes proof for all flux surface orientations in the original FRC.

In summary, we have shown through symmetry properties that adding to an FRC a small anti-symmetric (odd-parity) static magnetic field maintains closure of a closed flux surface. The closed field line undergoes expansion or contraction in the minor radial direction, if it does not lie in the plane perpendicular to $\mathbf{B}_{T-}$. It tilts in the toroidal direction, if it does not lie in the plane parallel to $\mathbf{B}_{T-}$. Numerical modeling will later show additional features: a well-defined separatrix continues to exist; some flux surfaces may "disappear" if they expand of contract beyond certain limits, X points may shift; or new nulls may appear.

The geometrical picture showed that, for a flux surface with *z-extremum* points *a* and *a'* at the nodes of B_{T-}, those points remain fixed with the addition of B_{T-}. If the axial extent of a flux surface is different from L, the periodicity length of the added field, then the procedure of Newcomb[14] must be followed to ascertain a field line's identity. The procedure is to start with zero B_{T-} field. Slowly turn it on, generating an electric field **E** according to Faraday's Law. Points on a field line move with a velocity $\mathbf{u} = \mathbf{ExB}/B^2$, which may be different at each point. As the transverse field approaches its desired strength, gradually stop the increase. The identity of the field line is thus followed. For a time-varying, $\ell = 1$, vacuum, transverse mode, one can readily show that though E_z is zero at $z\text{-}z_0 = \pm L/2$, E_r and E_ϕ are non-zero, thus the *extrema* will move. Certain plasma current distributions can make all components of **E** equal to zero at the *z extrema*. The motion of the field line at velocity **u** explains why some contracting field lines may disappear at the O-point or expanding ones may merge into the separatrix.

B. Graphing procedure: Symmetric mode

From the geometric argument in the last section, we can infer that the primary property of the transverse field which is essential to CP is a field-line-weighted zero average along the perimeter of the flux surface. Anti-symmetry is a sufficient condition to assure this. Anti-symmetric small-amplitude transverse modes are CP for flux surfaces inside the separatrix, hence globally. A symmetric transverse mode may be CP for a single flux surface, but not for all flux surfaces. Mode periodicity is not essential to CP, e.g., a mode $\propto (z\text{-}z_0)$ is adequate.

Performing CW and CCW 90° field-line-following procedures for the standard RMF mode, $\ell_+ = 0$, or an $\ell_+ = 1/2$ mode, Figure 6a), immediately shows that one cannot join field lines started at points *a* and *a'* to points *c* or *c'*. As shown in Figure 6b) for the $\ell_+ = 1/2$ case, following a field line 90° CW from point *a* and 90° CCW from *a'*, ends up at points *c2* and *c1* respectively. Alternately, following the net field line in 180° CW and 180° CCW directions from point *a*, results in reaching points *d2* and *d1*, respectively. The non-CP behavior for the 180° graphings originates in the lack of symmetry of the field line about the line $y = y_0$ and clearly shows the physical origin of the spiral shape described in Ref. 9 and 10 with linear-algebra techniques.

Transverse modes with helical symmetry are also of interest since they have already been used successfully in current-drive experiments.[15] For helical coils with a small pitch angle, $k_z L << 1$, the transverse part of the helical modes can be approximated by

$$B_x = B_{T-} \operatorname{Sin} k_z(z\text{-}z_0) = B_\tau \operatorname{Sin} k(z\text{-}z_0) \operatorname{Sin} k_z(z\text{-}z_0) \qquad (2a)$$

$$B_y = B_{T-} \operatorname{Cos} k_z(z\text{-}z_0) = B_\tau \operatorname{Sin} k(z\text{-}z_0) \operatorname{Cos} k_z(z\text{-}z_0) \qquad (2b)$$

While the B_y component remains anti-symmetric about $z = z_o$, the B_x component is now non-zero and symmetric about $z = z_o$. Field line opening will occur. Our numerical integration has confirmed this.

III. Numerical modeling of field-line structure

The numerical model is a predictor/corrector code that graphs (in both directions from a starting point) magnetic field lines defined by a Solov'ev equilibrium with different added fields. The Solov'ev equilibrium[13] can be described by a flux function, Ψ,

$$\Psi = K r^2 [1-(r/r_s)^2 - (z/z_s)^2] \qquad (3)$$

where r_s is the separatrix radius at $z = 0$, z_s is the X-point position, and K is a constant related to the field strength. The Solov'ev fields are

$$B_r = -2\,K\,r\,z/z_s^2 \qquad \text{and} \qquad (4a)$$

$$B_z = -2\,K[1 - 2(r/r_s)^2 - (z/z_s)^2]. \qquad (4b)$$

The equilibrium used for illustrations in this paper has $z_0 = 0$, $z_s = 2$, $r_s = 0.7$, and K = 0.5, corresponding to a prolate FRC with a magnetic field at the separatrix midplane of amplitude $B_z(r_s,0) = 1$.

A Solov'ev FRC field structure is shown approximately in Figure 1. We now demonstrate the effect on the field-line structure of the addition of a small ($B_T = 0.005$), uniform, symmetric ($\ell_+ = 0$) transverse field in the $\mathbf{e}_y$ direction, see Figure 7a). This transverse field has the same shape as studied in Ref. 9 and 10 and as used in rotamak experiments. The magnetic field line shown in red originates near the separatrix in a plane only 0.1° out of the *y-z* plane, the plane parallel to $\mathbf{B}_T$. Field lines this close to the *y-z* plane spiral in from their original position towards the magnetic null line of the O point. As they approach the null line, they move out of their original plane, spiral around the null line, and move nearly 180° towards a mirror-image plane. They then spiral out of the FRC in the opposite *z* direction from which they entered. The field line shown in blue also originated near the separatrix, but at 30° from the *y-z* plane. It, too, spirals away from its original plane, but at a much larger minor radius compared to the red field line. This difference occurs because of the larger component of the transverse field in the 30° plane compared with that in the 0.1° plane. Field lines precisely on the *y-z* plane (not shown) spiral onto the null line at the O point and never leave that plane, see Figure 4, Ref. 10. Our results confirm the open field structure in Refs. 9 and 10, showing the out-of-plane field-line motion in a direct clearer way. A field line may be very long, but there are no closed field lines, in the sense used in magnetic-fusion research.

Present-day RMF experiments have much larger B_T fields, typically 0.1 to 1 relative to the axial field strength of 1. For $B_T = 0.1$, a field line may not even make a single spiral around the null line before leaving the FRC, see Figure 7b). (The different classes of open field lines are discussed in Ref. 10.) Although field reversal is maintained,[7] this configuration is clearly not closed.

We now consider the anti-symmetric mode proven earlier to be CP. Figure 8a) shows the effects on flux surfaces in the y-z plane of the field shown in Figure 2, with amplitude $B_{T-} = 0.04$. As predicted by the graphical proof illustrated in Figure 4, flux

surfaces on one side of the *y-z* plane increase in enclosed area and those on the other side decrease in area. Most importantly, they remain closed. For these plots, the z extrema of the flux surfaces graphed had the same position as without the added field. Note that the flux surfaces change shape. Those with decreased area, at y > 0, develop a slight indentation near the z = 0 plane. For flux surfaces oriented perpendicular to the transverse field, Figure 8b) shows nearly no effect on the shape of the projection of flux surfaces originally in the x-z plane onto that plane. Tilt and curvature are evident when the flux surfaces are viewed edge on, see Figure 8c).

As the strength of the anti-symmetric field is increased, the O point in the upper y-z plane moves slightly radially inward. Field lines near that O point eventually compress sufficiently that reconnection occurs, forming two new nulls, see figure 9b). For the parameters used here, the new nulls first appeared at the O point at an amplitude of ~ 0.0477. That O point, at $y > 0$, continues to exist, as it shifts to slightly smaller radius with increasing transverse field strength. The two X points remain fixed at $z = z_s$ at $r = 0$.

The two new nulls are located at the centers of field-line spirals -see Ref. 10 and references therein for a discussion of spiral nulls- in symmetric positions across the $z = z_0 = 0$ plane. The positions of the two new nulls can be found by finding the zeroes of the sum of Equations 4) and 1). With increasing transverse-field amplitude, the new nulls move away from the original O-point position according to the proportionality,

$$z_n, (r_0 - r_n) \propto (B_t - B_{threshold})^{\alpha} , \qquad (5)$$

where $\alpha = 1$ for $(r_0 - r_n)$ and $\alpha = 1/2$ for z_n.

Figure 10) shows, in perspective, the field structure near the *y-z* plane of an $\ell = 1$ mode with amplitude 0.07. These field lines, originating near, but not in, the *y-z* plane, are seen top remain closed inside a well-defined separatrix. Field lines, which spiral into a new null move far from the original plane as they spiral in, cross the axial midplane and then move toward the other null, unspiral, and finally connect with themselves.

We have investigated several other anti-symmetric modes, such as i) $B_y \propto z$ and ii) $B_y \propto \text{Sin } z$. For both $\nabla \times \mathbf{B} \neq 0$. Case ii) behaves similarly to the 10-wire model, with two new spiral nulls forming. Case i) behaves quite differently. No new nulls appear. Instead the X points migrate up into the positive z-y plane. At an amplitude of ~ 0.11, the X points meet at the axial midplane.

IV. Summary

In summary, it has been found that a magnetic field that is anti-symmetric about the axial mid-plane can be added to a Solov'ev FRC and maintain its closed field-line structure. This is in stark contrast to earlier work (Refs. 5, 7, 9, and 10) in which the addition of a symmetric transverse field always opened all the field lines. These results could be very important for the RMF current-drive concept if new experiments show the opening of the FRC field lines to be detrimental, particularly for electron thermal losses. Small perturbations to either the FRC field or the transverse field can destroy the anti-symmetry. If the resulting symmetric components are small, the field line length is very long before it intersects a boundary, which may ameliorate particle and energy losses.

Acknowledgements

We thank A.H. Glasser, A.L. Hoffman, R. Mandelbaum, L. Steinhauer, and J.T. Slough for useful discussions. This work was supported in part by grants from the Office of Fusion Energy Sciences of the U.S. Department of Energy and Contract No. DE-AC02-76-CHO-3073.

References

[1] For a review, see M. Tuszewski, Nucl. Fusion 28, 2033 (1988).
[2] H.A. Blevin and P.C. Thonemann, Nucl. Fusion: Supplement, Part 1, 55 (1962).
[3] For a recent review, see I.R. Jones, Phys. Plasmas 6, 1950 (1999).
[4] G. Votroubek, J. Slough and E. Crawford, Bull. Amer. Phys. Soc. 43, 1766 (1998).
[5] S.W.H. Cowley, Radio Science 8, 903 (1973).
[6] W.N. Hugrass, I.R. Jones, K.F. McKenna, et al., Phys. Rev. Lett. 44, 1676 (1980).
[7] A.H. Boozer, Nucl. Fusion 18, 1663 (1978).
[8] P.M. Bellan, Phys. Rev. Lett. 62, 2464 (1989).
[9] P. Watterson, J. Plasma Physics 46, 271 (1991).
[10] M.S. Chance, J.M. Greene, and T.H. Jensen, Geophys. Astrophys. Fluid Dynamics 65, 203 (1992).
[11] S.A. Cohen and A.H. Glasser, in preparation.
[12] S.A. Cohen, Bull. Amer. Phys. Soc. 44, 586 (1999).
[13] L.S. Solov'ev, Rev. Plasma Phys. 6, 239 (1976).
[14] W.A. Newcomb, Ann. Phys. N.Y. 3, 347 (1958).
[15] M.J. Dutch and A.L. McCarthy, Physics Letters A 122, 165 (1987).

Figure captions

1. Schematic of an FRC. A set of coils in a solenoidal array forms an axial field. Toroidal current in the FRC generates a set of closed, poloidal, nested field lines. The separatrix defines the boundary between closed flux surfaces and open ones. A transverse magnetic field may exist across an FRC, perhaps formed by external coils or by the earth's field. Transverse fields with gradients may have a component parallel to the axial field or in the toroidal direction.

2. a) Plot of the anti-symmetric (odd parity) magnetic field, B_{T-}, formed by a set of 5 pairs of current-carrying wires, oriented perpendicular to the *y*-*z* plane, see Figure 3. b) Dependence on axial position of the amplitude of the transverse and parallel components of B_{T-}.

3. Orientation of 5 pairs of parallel wires used to create the anti-symmetric field shown in Figure 2. A pair consists of two parallel wires on diametrically opposite sides of the FRC. The relative amplitudes of the currents in each pair of wires are indicated.

4. a) Axial variation of an anti-symmetric field, with transverse component in the *y* direction only. b) Addition of the anti-symmetric field shown in a) maintains the closedness of the flux surface. A closed FRC flux surface (solid line) in the upper *y*-*z* plane expands in enclosed area (dashed line), with the addition of this anti-symmetric field. c) Field components of the FRC, $\mathbf{B}_s$, and the added field, B_τ and B_π, (transverse and parallel parts, respectively), at point *e* and, d) at point *e'*. e) reversing the field components at e', is necessary for the CCW graph shown in a). f) A closed FRC flux surface (solid line) in the lower *y*-*z* plane decreases in enclosed area (dashed line) when the field in a) is added.

5. a) Effect on an FRC closed flux surface lying in the plane normal to the anti-symmetric transverse field shown in Figure 2a). To first order, the flux surface simply tilts out of the plane. b) and c) Field components of the FRC, $\mathbf{B}_s$, and the added field, B_τ and B_π, the transverse and parallel parts respectively, at points *e* and *e'*. d) reversing the field components at e', to compare with b) and to accomplish the CCW segment of the graph in a).

6. a) Axial variation of the $\ell_+ = 1/2$ symmetric transverse field. b) Both 90° and 180° graphs of the net field (the sum of $\mathbf{B}_s$, B_τ and B_π) show the structure to spiral open.

7. a) A small-amplitude ($B_y = 0.005$), uniform ($\ell_+ = 0$), transverse magnetic field is added to a Solov'ev FRC. The red field-line originates at (-0.00122, -0.7, 0.0), 0.1º off the *y*-*z* plane. The blue field line originates at (-.35, -.606, 0), about 30º from the y-z plane. Though both field lines are long, they are clearly open. b) A larger amplitude ($B_y = 0.1$) uniform ($\ell_+ = 0$) transverse magnetic field is added to a Solov'ev FRC. The red field lines originate on the *x*–axis at x = -0.6, 0, 0.6, and y = z = 0. The blue field lines originate on the *y*–axis at y = -0.6, 0, 0.6, and x = z = 0.

8. Magnetic field lines when an anti-symmetric (ℓ = 1) transverse magnetic field (see Figure 2) of amplitude B_y = 0.04 is added to a Solov'ev FRC. a) Flux surfaces in the *y*–*z* plane show expansion and contraction. b) Projection of field lines originally in *x*–*z* plane onto that plane show little change in shape. c) Flux surfaces lines from b) show tilt and curvature when projected onto the x-y plane.

9. Magnetic field-lines in the *y*-*z* plane, for different-amplitude anti-symmetric ℓ = 1 transverse magnetic fields (see Figure 2) added to a Solov'ev FRC. a) B_y = 0.045, b) B_y =0.050, c) B_y = 0.06, d) B_y = 0.075, e) B_y =0.1, and f) B_y = 0.25. Above an amplitude of ~0.477, some field lines spiral into two new nulls, displaced symmetrically about the z = 0 plane.

10. For an anti-symmetric, ℓ = 1 mode with B_y = 0.07, a 3D – projection of magnetic flux surfaces, initialized with a small *x* value (0.001), to move them out of the *y* - *z* plane. As some magnetic field lines spiral in to one of the nulls, they lift out of the plane, move toroidally around the FRC, over to the other null, before spiraling back out and closing on themselves.

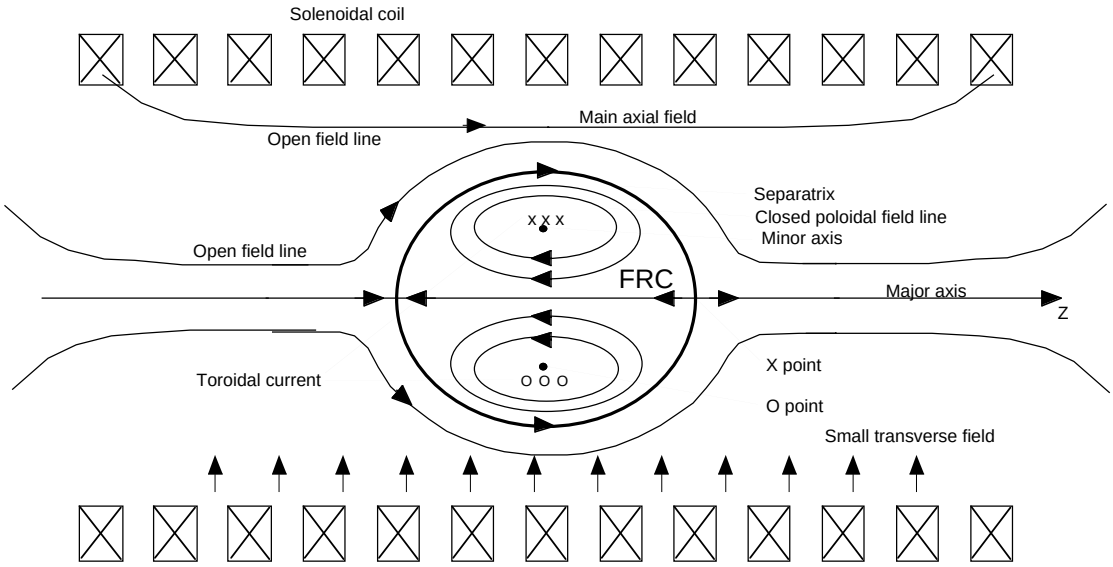

Figure 1. Schematic of an FRC. A set of coils in a solenoidal array forms an axial field. Toroidal current in the FRC generates a set of closed, poloidal, nested field lines. The separatrix defines the boundary between closed flux surfaces and open ones. A transverse magnetic field may exist across an FRC, perhaps formed by external coils or by the earth's field. Transverse fields with gradients may have a component parallel to the axial field or in the toroidal direction.

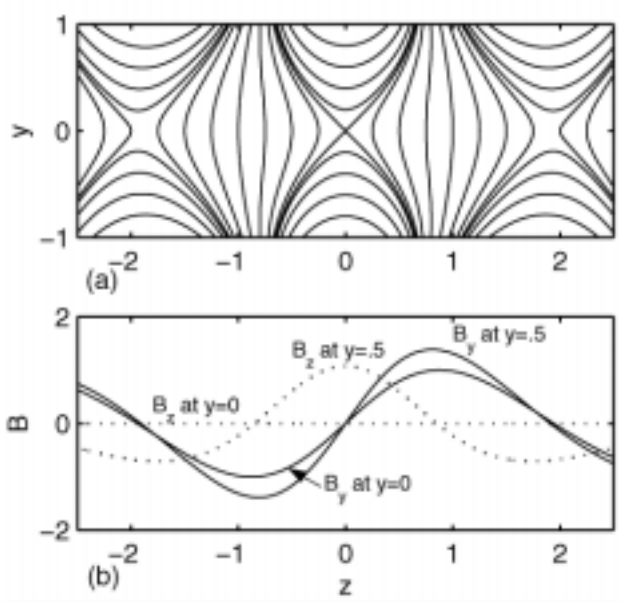

Figure 2. (a) Plot of the anti-symmetric (odd parity) magnetic field, B_{T-}, formed by a set of 5 pairs of current-carrying wires, oriented perpendicular to the *y*-*z* plane, see Figure 3. (b) Dependence on axial position of the amplitude of the transverse and parallel components of B_{T-}.

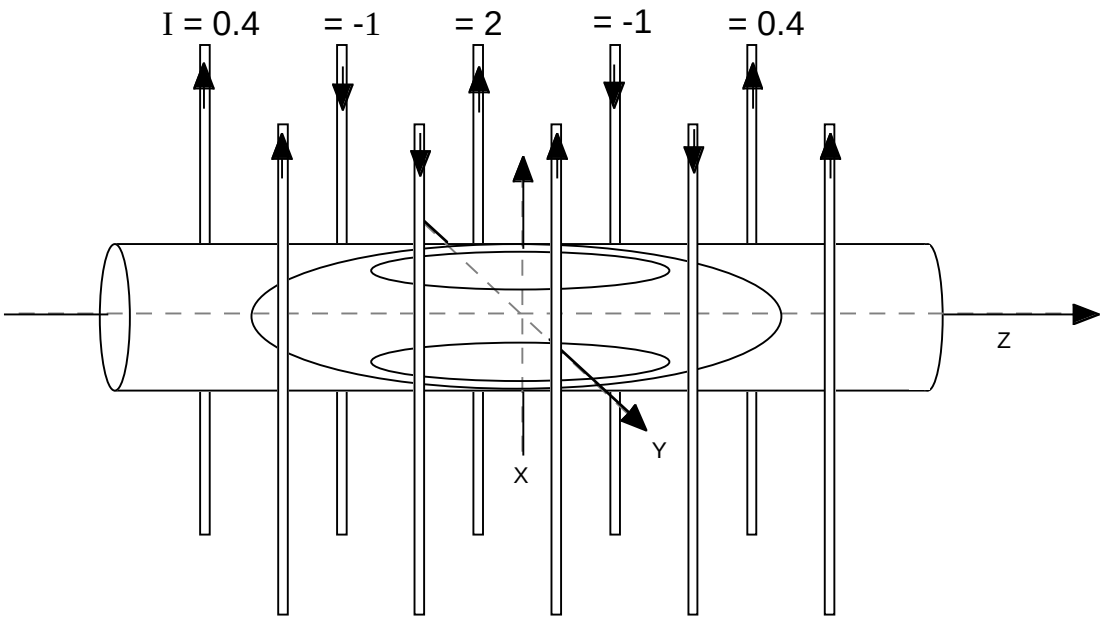

Figure 3. Orientation of 5 pairs of parallel wires used to create the anti-symmetric field shown in Figure 2. A pair consists of two parallel wires on diametrically opposite sides of the FRC. The relative amplitudes of the currents in each pair of wires are indicated.

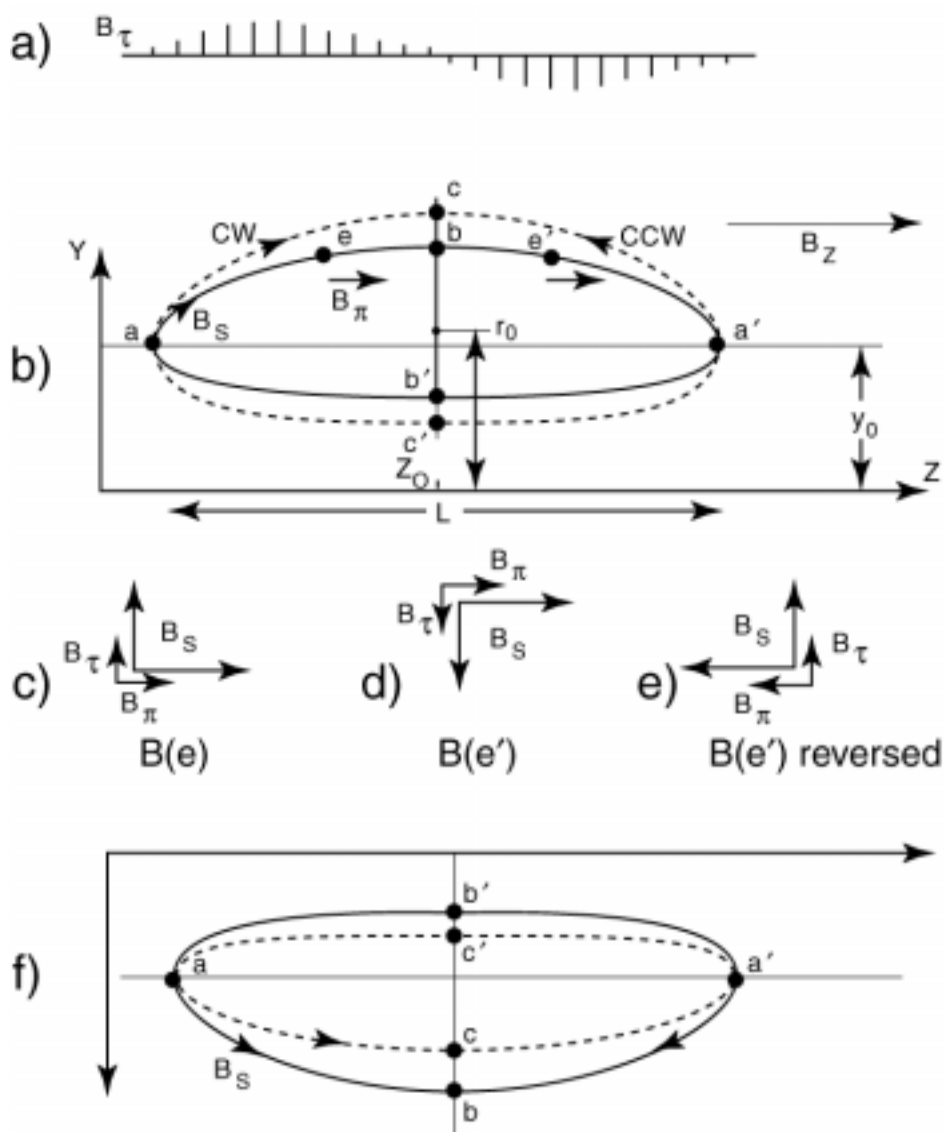

Figure 4. (a) Axial variation of an anti-symmetric field, with transverse component in the *y* direction only. (b) Addition of the anti-symmetric field shown in (a) maintains the closedness of the flux surface. A closed FRC flux surface (solid line) in the upper *y*-*z* plane expands in enclosed area (dashed line), with the addition of this anti-symmetric field. (c) Field components of the FRC, $\mathbf{B}_s$, and the added field, B_τ and B_π, (transverse and parallel parts, respectively), at point *e* and, (d) at point *e'*. (e) reversing the field components at e', is necessary for the CCW graph shown in (a). (f) A closed FRC flux surface (solid line) in the lower *y*-*z* plane decreases in enclosed area (dashed line) when the field in (a) is added.

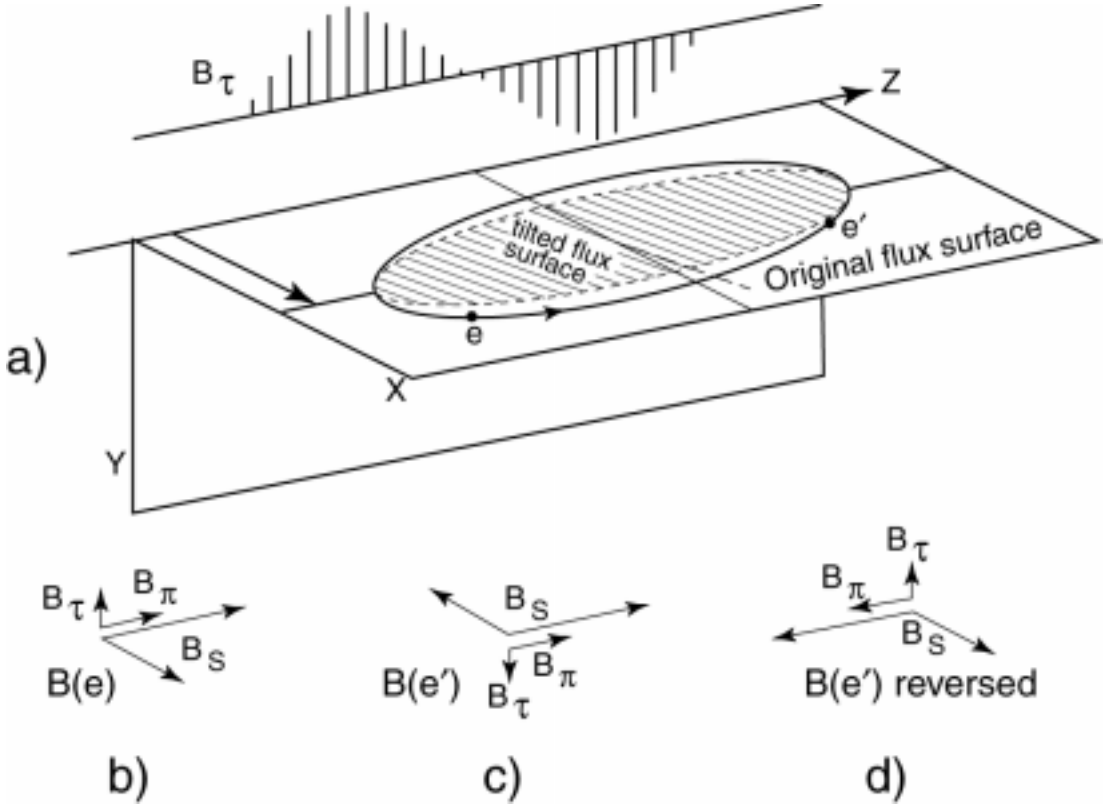

Figure 5. (a) Effect on an FRC closed flux surface lying in the plane normal to the anti-symmetric transverse field shown in Figure 2(a). To first order, the flux surface simply tilts out of the plane. (b) and (c) Field components of the FRC, $\mathbf{B}_s$, and the added field, B_τ and B_π, the transverse and parallel parts respectively, at points *e* and *e'*. (d) reversing the field components at e', to compare with (b) and to accomplish the CCW segment of the graph in (a).

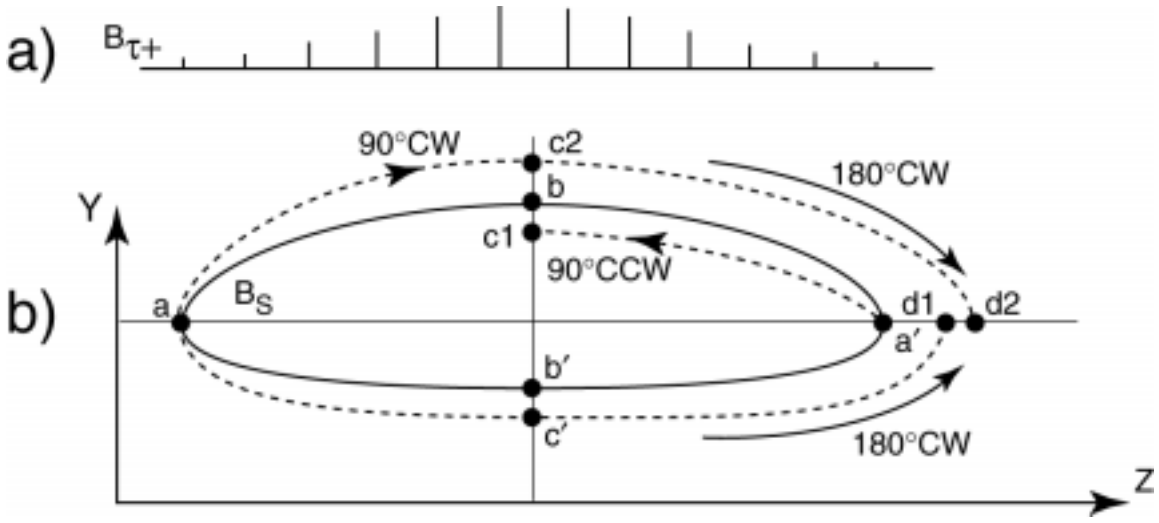

Figure 6. (a) Axial variation of the $\ell_+ = 1/2$ symmetric transverse field. (b) Both 90° and 180° graphs of the net field (the sum of $\mathbf{B}_s$, B_τ and B_π) show the structure to spiral open.

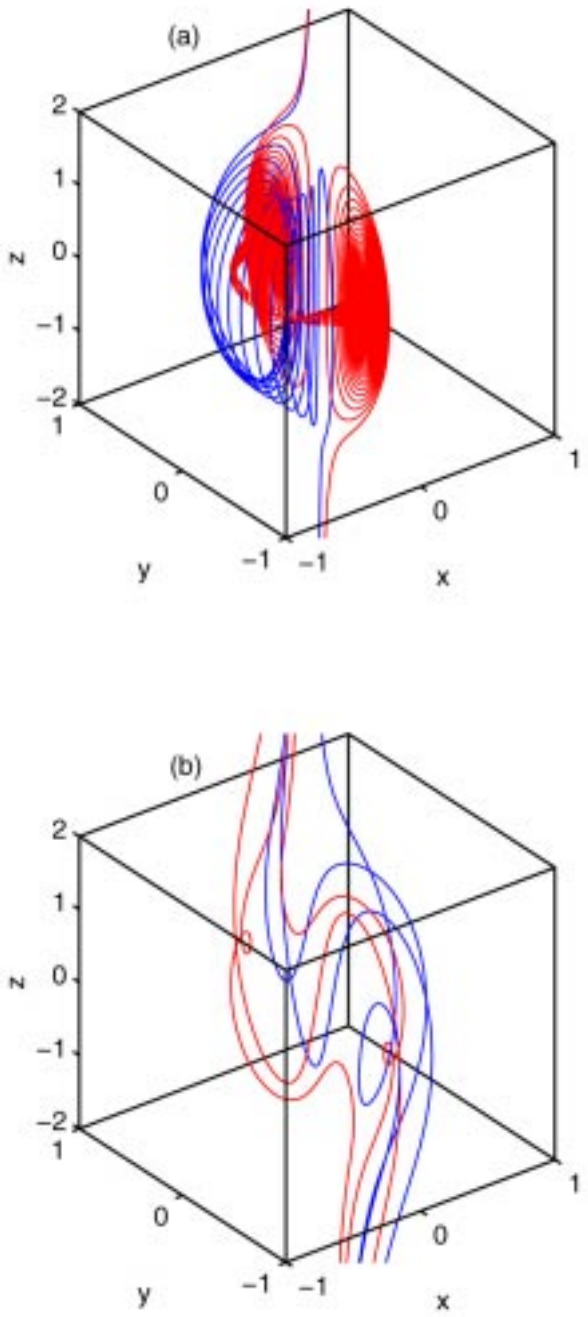

Figure 7. (a) A small-amplitude (B_y = 0.005), uniform (ℓ_+= 0), transverse magnetic field is added to a Solov'ev FRC. The red field-line originates at (-0.00122, -0.7, 0.0), 0.1° off the *y*-*z* plane. The blue field line originates at (-.35, -.606, 0), about 30° from the y-z plane. Though both field lines are long, they are clearly open. (b) A larger amplitude (B_y = 0.1) uniform (ℓ_+= 0) transverse magnetic field is added to a Solov'ev FRC. The red field lines originate on the *x*–axis at x = -0.6, 0, 0.6, and y = z = 0. The blue field lines originate on the *y*–axis at y = -0.6, 0, 0.6, and x = z = 0.

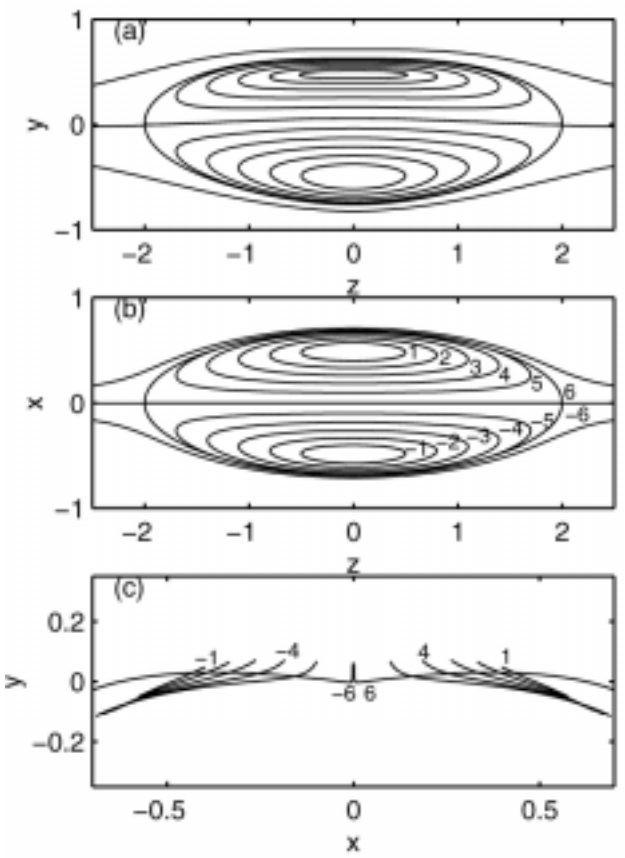

8. Magnetic field lines when an anti-symmetric ($\ell = 1$) transverse magnetic field (see Figure 2) of amplitude $B_y = 0.04$ is added to a Solov'ev FRC. (a) Flux surfaces in the *y*–*z* plane show expansion and contraction. (b) Projection of field lines originally in *x*–*z* plane onto that plane show little change in shape. (c) Flux surfaces lines from b) show tilt and curvature when projected onto the x-y plane.

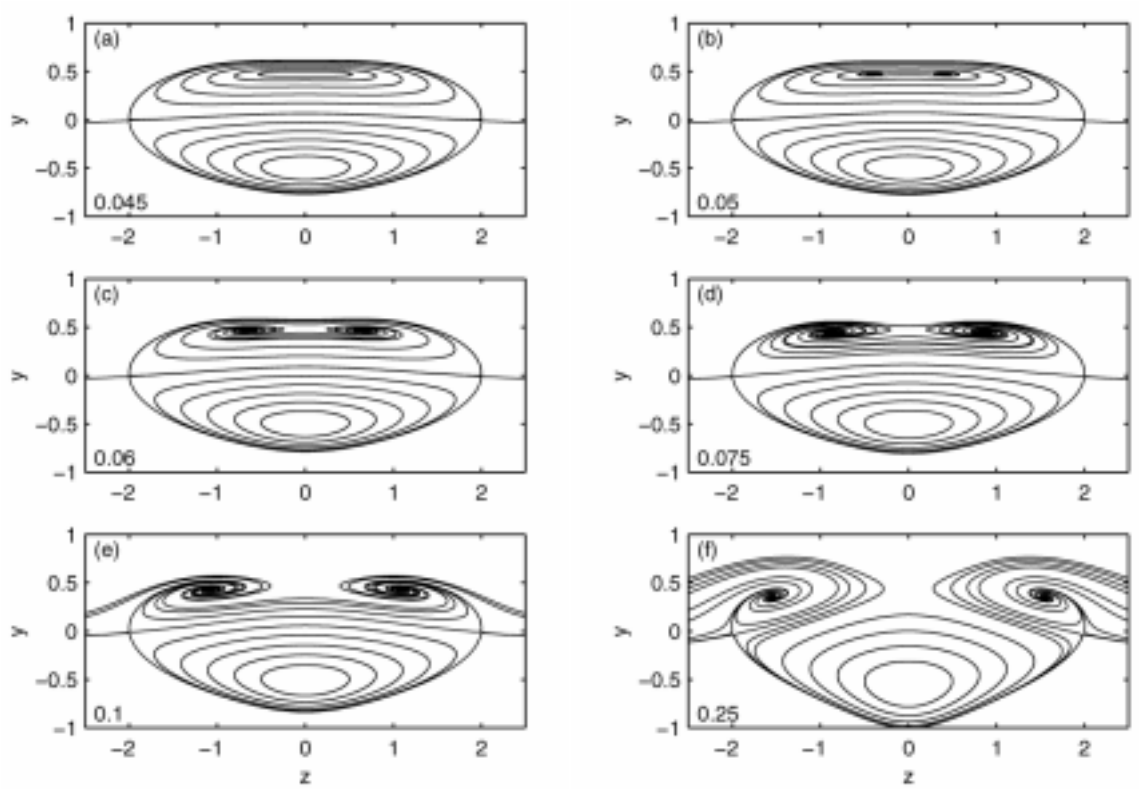

Figure 9. Magnetic field-lines in the *y*-*z* plane, for different-amplitude anti-symmetric $\ell = 1$ transverse magnetic fields (see Figure 2) added to a Solov'ev FRC. (a) $B_y = 0.045$, (b) $B_y = 0.050$, (c) $B_y = 0.06$, (d) $B_y = 0.075$, (e) $B_y = 0.1$, and (f) $B_y = 0.25$. Above an amplitude of ~0.477, some field lines spiral into two new nulls, displaced symmetrically about the z = 0 plane.

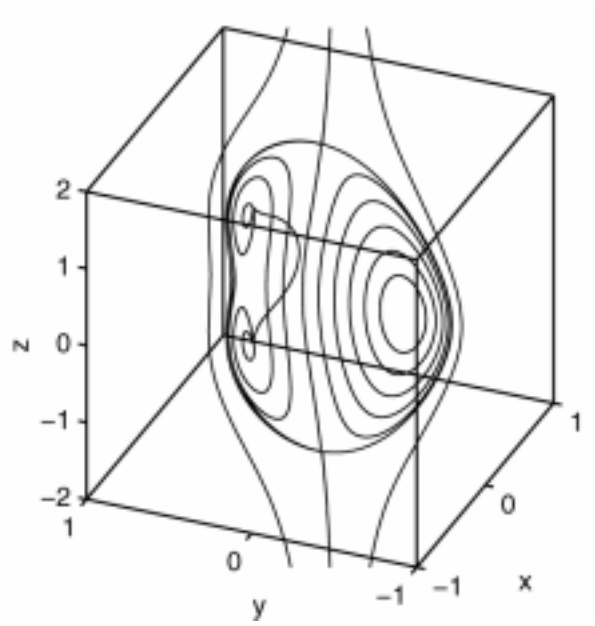

Figure 10. For an anti-symmetric, $\ell = 1$ mode with $B_y = 0.07$, a 3D – projection of magnetic flux surfaces, initialized with a small x value (0.001), to move them out of the y - z plane. As some magnetic field lines spiral in to one of the nulls, they lift out of the plane, move toroidally around the FRC, over to the other null, before spiraling back out and closing on themselves.